INFILL-FRAME INTERACTION: REFINED MODELLING FOR THE ANALYSIS AND THE ESTIMATION OF THE INTERNAL FORCES IN SEISMIC ASSESSMENT OF RC BUILDING

Available online at www.eccomasproceedia.org
Eccomas Proceedia COMPDYN (2023) 2882-2893

ECCOMAS
Proceedia

COMPDYN 2023
9th ECCOMAS Thematic Conference on
Computational Methods in Structural Dynamics and Earthquake Engineering
M. Papadrakakis, M. Fragiadakis (eds.)
Athens, Greece, 12-14 June 2023

INFILL-FRAME INTERACTION: REFINED MODELLING FOR THE ANALYSIS AND THE ESTIMATION OF THE INTERNAL FORCES IN SEISMIC ASSESSMENT OF RC BUILDING STRUCTURES

Fabio Di Trapani[1], Marilisa Di Benedetto[1], Massimo Petracca[2], Guido Camata[3]

[1] Dipartimento di Ingegneria Strutturale, Edile e Geotecnica, Politecnico di Torino
Corso Duca degli Abruzzi 24, 10129, Turin, Italy
fabio.ditrapani, marilisa.dibenedetto@polito.it

[2] ASDEA Software Technology
Via Alide Breviglieri 8, Pescara, Italy
m.petracca@asdea.net

[3] Dipartimento di Ingegneria e Geologia, Università degli studi "G. D'Annunzio" di Chieti-Pescara
Viale Pindaro 42, Pescara, Italy
g.camata@unich.it

Abstract

The paper deals with the assessment of the internal force distribution in frame members due to masonry infills interaction under seismic loads. Special interest is addressed to shear demand, which cannot be evaluated by the common equivalent strut models, while refined finite element modelling is not computationally effective to be used in practice. With the aim to maintain the simplicity of the equivalent strut approach for the assessment of existing RC structures, the paper presents a detailed study of the infill-frame shear transfer mechanism. Refined 2D nonlinear models of real experimental tests on infilled frames have been defined using the OpenSees / STKO software platform. Shear demands at the columns ends of different case study tests have been extracted by integrating the nodal forces at specific section cuts of the RC members. An analytical relationship is finally proposed to correct the shear demand at the ends of the columns when using the equivalent strut approach. The new formula relates the additional shear demand to the current axial force on the equivalent struts and the geometrical and mechanical properties of the infilled frames. The formula is thought to be easily used to perform step-by-step shear safety checks in seismic safety assessments of existing RC structures.

Keywords: Infilled frames, Shear, Masonry, Reinforced concrete, OpenSees, STKO.

ISSN:2623-3347
Peer-review under responsibility of the organizing committee of COMPDYN 2023.
doi: 10.7712/120123.10607.21394

1 INTRODUCTION

The interaction between infill and frame has been explored by researchers worldwide since the mid-20th century [1-5]. The complex contact interfacing between the infill and the surrounding frame members makes the behaviour under seismic loads highly nonlinear, posing a challenge for accurate prediction of the actual distribution of the internal forces in the frame members. Despite noteworthy advances of research on the topic [6-12], the assessment of the internal forces is still an object of investigation, as the accurate prediction of potential local shear failures [13-16] (Fig.1) is decisive to the assessment and the design of effective retrofitting interventions.

Figure 1: Local shear failure at column ends of infilled RC frames.

Numerical modelling techniques such as micro-modelling and macro-modelling approaches have been generally used for this purpose (Mehrabi et al. 1997 [7]; Di Trapani et al. [17]; Di Trapani et al. [18]). Micro-modelling methods allow simulating the behaviour of an infilled frame with a high level of accuracy, clearly highlighting the damage mechanisms as well as the localization of the stresses on the frame and on the infills. On the contrary, macro-models are simple and computationally effective, but since they are phenomenological models, they are useful to provide an estimation of the overall response, without predicting local interaction effects.

In this context, this study firstly provides a high-fidelity numerical micro-model of an infilled reinforced concrete (RC) frame using OpenSees [19] in combination with the Scientific ToolKit for OpenSees (STKO) [20] pre and post-processing suite. The micro-model provides continuum elements for masonry units, mortar, and RC members. Frictional interfaces are used to model the contact of the infill with the surrounding frame. The model is validated with the experimental results in terms of force-displacement response and failure mechanism. The distribution of the internal forces on the frame members is then obtained via numerical integration of the nodal forces at the different cross-sections. In the second step, the same tests were simulated using the equivalent strut approach. A simple analytical relationship is finally defined to predict the rate of the equivalent strut axial force, the is transferred as demand at the ends of the columns.

2 REFINED FE MICRO-MODELLING OF THE INFILLED FRAME

2.1 Modelling strategy

The micro-model employs a 2D continuum damage model, which allows for the simulation of the non-linear behaviour of masonry components (units and mortar) as well as concrete members. The model was arranged with the STKO software platform [20] which implements

OpenSees as a solver. Both the frame and the masonry were modelled using 2D *quadrilateral* elements. A scheme of the modelling approach is depicted in Fig. 2.

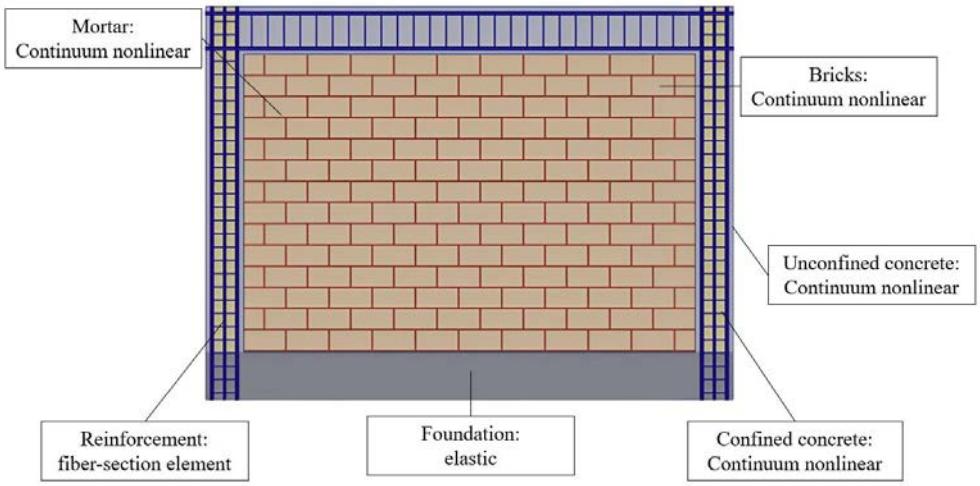

Figure 2: 2D Micro-model of the infilled-frame in OpenSees / STKO

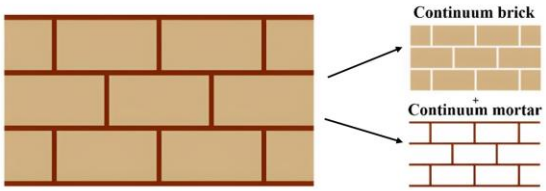

Figure 3: Masonry continuum micro-model

Masonry units and mortar were modelled as separate continuous elements (Fig. 3). The *DamageTC3D* constitutive model (Petracca et al. [21]) was used to model the nonlinear response and the damage evolution. This constitutive model is based on a continuum damage mechanism, which involves a tension-compression damage law, where the stress tensor σ is defined as follows (Eq.1) [21]:

$$\sigma = (1-d^{+})\bar{\sigma}^{+} + (1-d^{-})\bar{\sigma}^{-} \tag{1}$$

in which σ represents the nominal stress tensor, while σ^{+} and σ^{-} are the positive and negative parts of the effective stress tensors, respectively [21]. The damage indices d^{+} and d^{-} are based on the tensile and compressive laws of masonry units and mortar, which can be evaluated through the stress-strain curves of the material. According to this material constitutive law [21], fracture energy must be defined for the material. The latter accounts for the amount of energy required to propagate a crack per unit length. The fracture energy in tension (G_t) and compression (G_c) is here estimated according to Model Code 2010 [22] formulation, that is:

$$G_t = 0.073 \cdot f_c^{0.18} \tag{2}$$

$$G_c = \left(\frac{f_c}{f_t}\right)^2 \cdot G_t \tag{3}$$

where f_c and f_t are each time the tensile and compression strengths of the materials. The reinforced concrete elements are modelled as continuous 2D quadrilateral elements and the

ASDConcrete3D constitutive model was applied to the concrete frame members. The latter is an upgraded version of *DamageTC3D*, which is more capable in capturing the damage in concrete elements [19, 20].

Rebars are modelled as 1D *force beam-column* elements (Fig. 4b) embedded in the concrete elements. The uniaxial material model *Steel02* was used as constitutive model. The embedment condition of the rebars within the concrete elements is realized by defining the node-to-element links using the *ASDEmbedded Node Element* as depicted in Figure 4b. Finally, *zero-length* contact elements transferring normal contact forces and shear frictional forces are used to simulate the behaviour of the interface between the RC frame and the masonry infill panel (Fig. 4a).

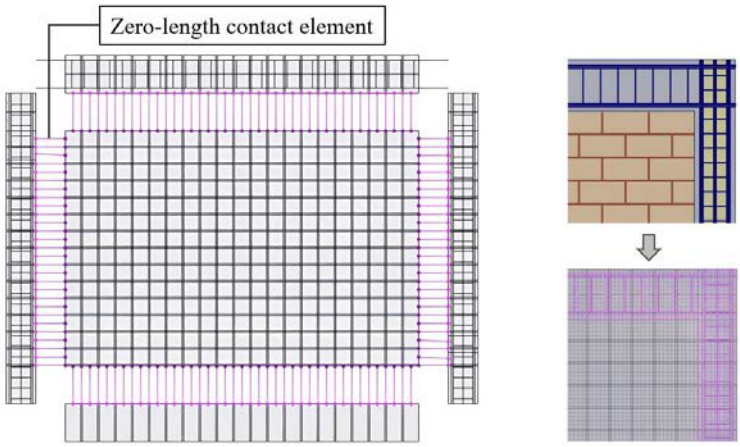

Figure 4: (a) Frame-infill contact interface model (b) Reinforcement detail and node-to-element links (embedded rebars in concrete)

2.2 Details of the selected specimens

The proposed micro-modelling approach was applied to simulate four reference experimental tests on masonry-infilled frames. These tests were chosen from the experimental campaigns by Mehrabi and Shing [6] and Cavaleri and Di Trapani [2], with the goal of providing as much coverage as possible of various masonry infill typologies. Infill walls of specimens S8 and S9 from Mehrabi and Shing [6] were made by hollow clay brick masonry (8) and solid clay brick masonry (9). Infills of specimens S1A and S1B by Cavaleri and Di Trapani [2] were arranged with solid calcarenite and hollow clay masonry units, respectively.

The specimens by Mehrabi and Shing [6] experimental were tested to lateral monotonic loads with a constantly applied vertical load. Specimens S8 and S9 were subjected to a vertical load of 97.9 kN acting on the beam and 97.9 kN acting on each column. Specimens S1A and S1B by Cavaleri and Di Trapani [2] were subjected to a constant vertical load of 200 kN on each column, and then tested under cyclic load conditions. A summary of the main features of the reference experimental tests is provided in Table 1. mechanical properties of materials are also outlined in Tables 2 and 3.

Reference	Specimen ID	Masonry type	Infill length (*l*) [mm]	Infill height (*h*) [mm]	Aspect ratio (*l*/*h*) [-]
Mehrabi & Shing [6]	S8	Hollow clay bricks	2134	1422	1.5
	S9	Solid clay bricks	2134	1422	1.5
Cavaleri & Di Trapani [2]	S1A	Solid calcarenite units	1600	1600	1.0
	S1B	Hollow clay units	1600	1600	1.0

Table 1: General details of selected infilled frame specimens.

Specimen	Concrete		Units		Mortar
	Elastic modulus [MPa]	Compressive strength [MPa]	Compressive strength ($f_{b,v}$) [MPa]	Compressive strength ($f_{b,h}$) [MPa]	Compressive strength [MPa]
S8	17225	26.8	16.48	8.51	8.01
S9	17225	26.8	15.57	-	12.47
S1A	25500	25	7.06	-	3.06
S1B	25500	25	37.68	2.06	9.16

Table 2: Mechanical properties of concrete, masonry units and mortars of selected infilled frame specimens.

2.3 Model validation

Two steps were taken to carry out the analyses. First vertical loads were applied and kept constant. In the second phase, the horizontal monotonic load was applied. The lateral force versus lateral displacement responses from the micro-models were then compared to the positive and negative experimental monotonic envelopes (Fig.5). The latter show a satisfactory agreement both in terms of peak resistance, stiffness, and post-peak decay.

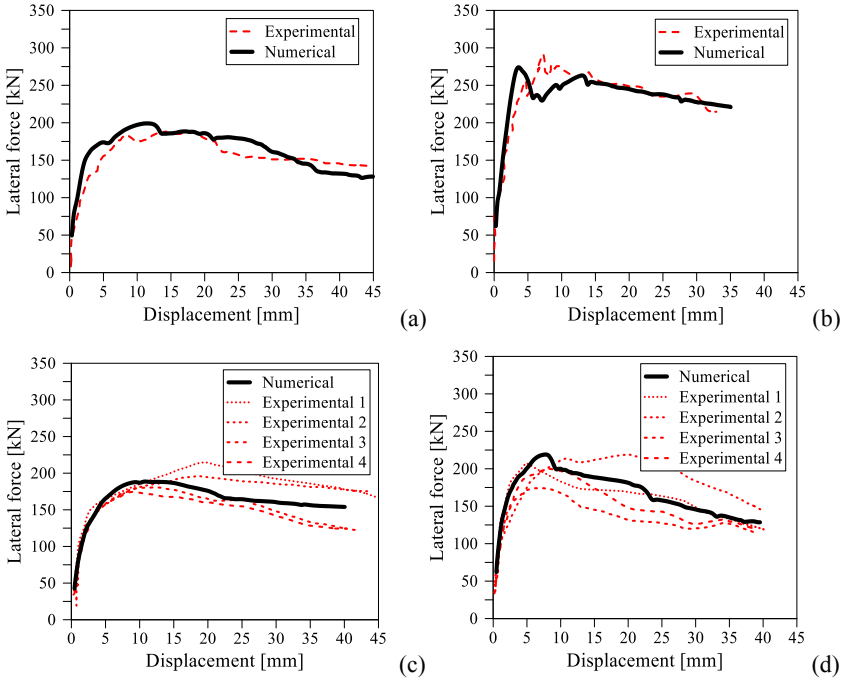

Figure 5: Comparison between experimental and numerical response:(a) S8 (b) S9 (c) S1A (d) S1B

In Fig.6 and Fig.7, experimental and numerical damage patterns are also compared. As it can be observed, the numerical models were also able to accurately predict the main cracking patterns in the masonry (bricks and mortar joints) as well as reinforced concrete elements (shear and flexural damage) in this case.

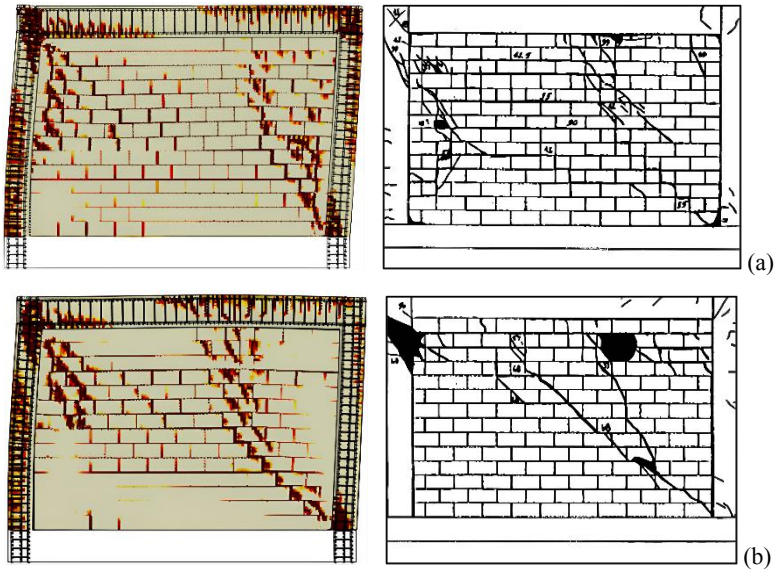

Figure 6: Numerical vs. Experimental damage pattern comparisons for Mehrabi and Shing [6]: (a) Specimen 8; (b) Specimen 9.

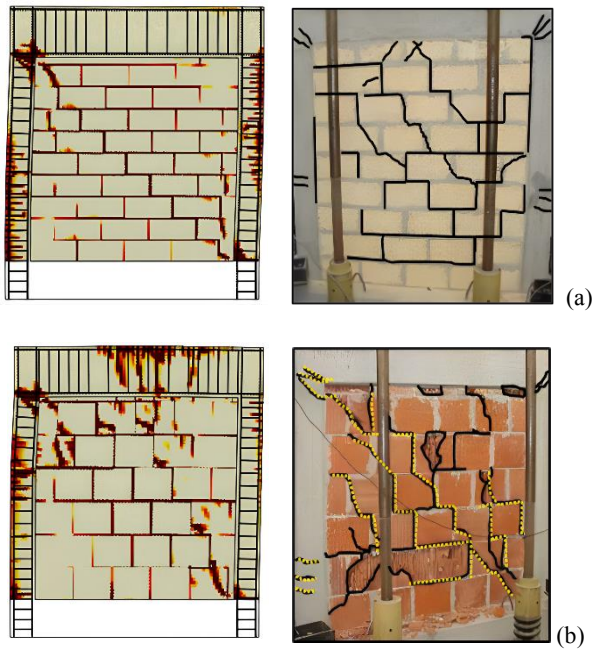

Figure 7: Numerical vs. Experimental damage pattern comparisons for Cavaleri and Di Trapani [2]: (a) Specimen S1A; (b) S1B.

3 EVALUATION OF THE INTERNAL FORCES DISTRIBUTION

The evaluation of the internal force has been carried out by implementing a TCL script in the STKO post-processing module. The latter allows the definition of a node set and collecting the nodal forces. The forces are then integrated across the defined section, called "section cut". As depicted in Figure 8, a total number of twenty section cuts was defined to reproduce the internal forces distribution over the concrete frame. A refinement of the section cuts was provided from the midspan to the ends of the columns, where it is expected the major force transfer, and so the major variability of the internal forces in the frame members.

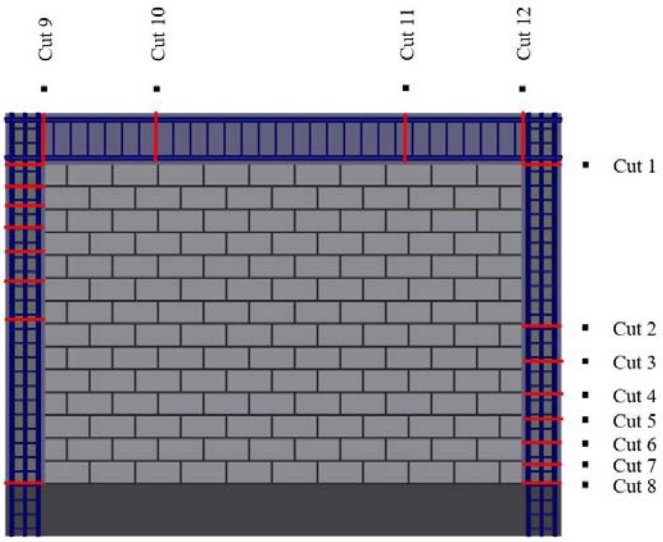

Figure 8: Section cuts' definition for RC frame

The internal forces were recorded at each step of the analysis. For the sake of brevity, only the shear demand distributions are here reported. In particular, three stages of the analysis are represented in Figures 9 and 10, namely those corresponding to the initial cracking, the peak resistance, and the final stage of analysis.

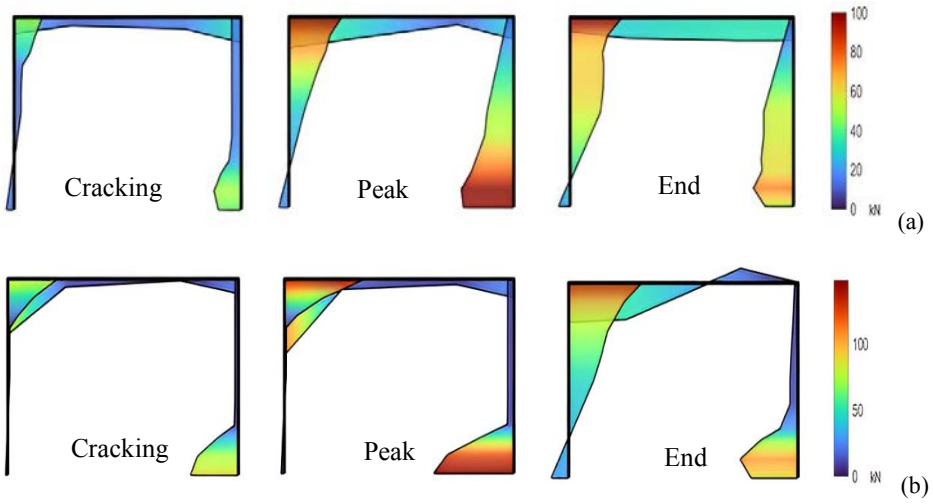

Figure 9: Shear demand distribution in frame members for Mehrabi and Shing [6] specimens: (a) S8; (b) S9.

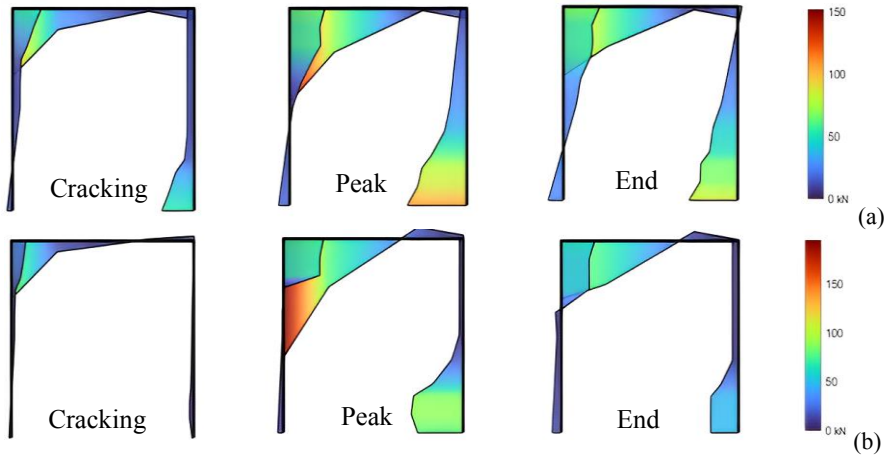

Figure 10: Shear demand distribution in frame members for Cavaleri and Di Trapani [2] specimens: (a) S1A; (b) S1B.

The evolution of shear force experienced by the selected infilled frame specimens was partially consistent with the findings of previous studies (e.g. D'Ayala et al. 2009 [23], Cavaleri and Di Trapani 2015 [24], Bolis et al. 2017 [25], Milanesi et al. 2018 [16]), generally highlighting a noticeable increase of shear demand of at the ends of beams and column. However, it has been found that such a shear demand increment at the ends is not always so pronounced. In fact, some cases (e.g. S8 or S1A) have shown a shear diagram that is linear throughout the entire column. This occurrence can be justified by the increase of the contact length which occurs because of a major sliding of the mortar joints, and that could be captured by the enhanced micro-model because of the physical modelling of the mortar joints. The section nodal forces integration was additionally used to assess the base shear demand of the individual components of the infilled frames. The sum of the shear demands at the base cross sections of the columns provided the lateral response of the RC frame coupled with the infill. By subtracting th so evaluated contribution of the frame from the overall response, the actual contribution of the infill is isolated. Results displaying the base shear-displacement curves by elements are illustrated in Fig. 11 for the analyzed specimens.

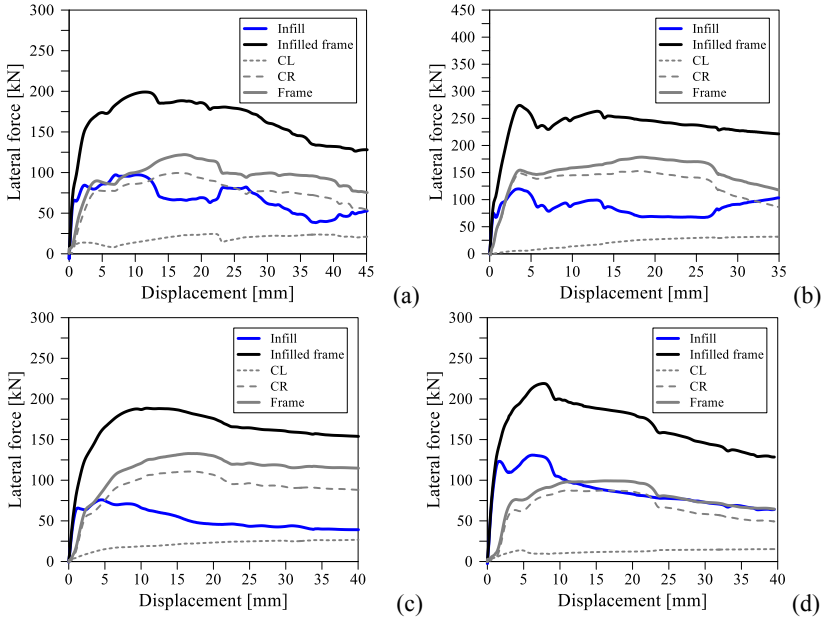

Figure 11: Shear demand in infilled-frame components: (a) S8 (b) S9 (c) S1A (d) S1B

4 EVALUATION OF THE ADDITIONAL SHEAR DEMAND USING MACRO-MODELLING

Equivalent strut macro-models do not allow assessing the local shear demand due to the interaction between the frame and the infill. In order to formulate a predictive analytical model it can be assumed (Fig.12a) that the total shear demand at the end of a column adjacent to the infill ($V_{d,tot}$) is the sum of the drift-induced shear on the frame ($V_{d,frame}$) and the extra shear demand arising from the frame-infill interaction ($V_{d,inf}$), as follows:

$$V_{d,tot} = V_{d,frame} + V_{d,\inf} \tag{4}$$

While $V_{d,frame}$ is already available as the shear internal force from the frame, the term $V_{d,inf}$ is unknown. However it can be reasonably assumed the shear force $V_{d,inf}$ is a rate of the axial force acting on the equivalent strut. In fact, considering the forces acting on a portion of infill at the end of a column, the translational equilibrium equation provides:

$$V_{d,\inf} = N\cos\theta - T \tag{5}$$

This implies that the extra amount of shear demand is the difference between the horizontal component of the axial force on the strut and the friction force at the interface, denoted as T. The latter is related to the vertical component (σ_v) of the normal stress acting on the strut (σ_v) through the friction coefficient (μ) and acts on a contact length (αl), which is a portion of the total length of the infill (αl, with $\alpha \leq 1$). The tangential force at the interface is therefore:

$$T = \mu \cdot \sigma_v \cdot t \cdot \alpha l \qquad \sigma_v = \sigma_n \sin\theta \;;\; \sigma_n = N / w \cdot t \tag{6}$$

By substituting Eq. (6) in Eq. (5) it follows:

$$V_{d,\inf} = N\cos\theta - \mu\sigma_n \sin\theta \cdot t \cdot \alpha l = N\cos\theta - \frac{\mu \cdot N \sin\theta \cdot t \cdot \alpha l}{w \cdot t} = N\left(\cos\theta - \frac{\mu \cdot \sin\theta \cdot \alpha l}{w}\right) \tag{7}$$

providing the additional shear demand as a function of the contact length (αl) and the current axial force (N) on the corresponding strut.

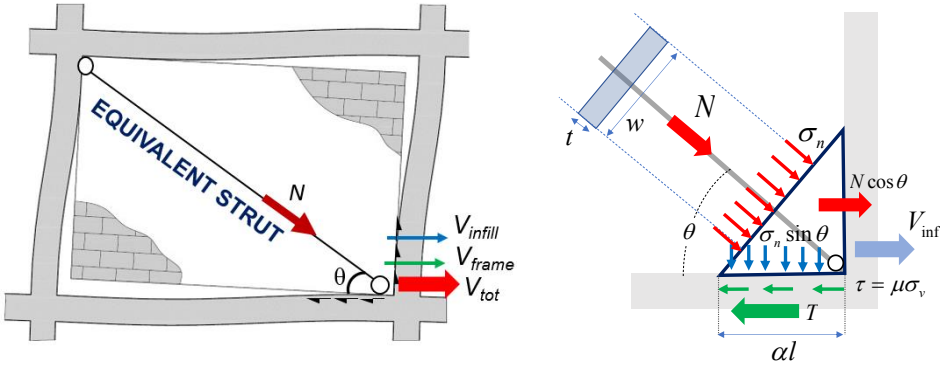

(a) (b)

Fig. 12: (a) Shear demand decomposition at the end of the columns of an infilled RC frame (b) Force transmission due to frame-infill interaction.

The validity Eq. (4) coupled with Eq. (7) has been tested by modelling the specimens mentioned according to using the macro-modelling approach suggested by Di Trapani et al. [18]. Figures 13 and 14 report the outcomes of the implementation of the proposed analytical model to adjust the shear demand, in comparison with the actual shear demand derived from the micro-model. A noticeable consistency with the results from the refined micro-model is ob-

served despite the simplicity of the analytical formulation. As regards the contact lengths, it was estimated that for the windward and leeward columns, αl=0.30·l and 0.4·l for l/h=1, and αl =0.25· l and 0.3· l for l/h=1.5, respectively.

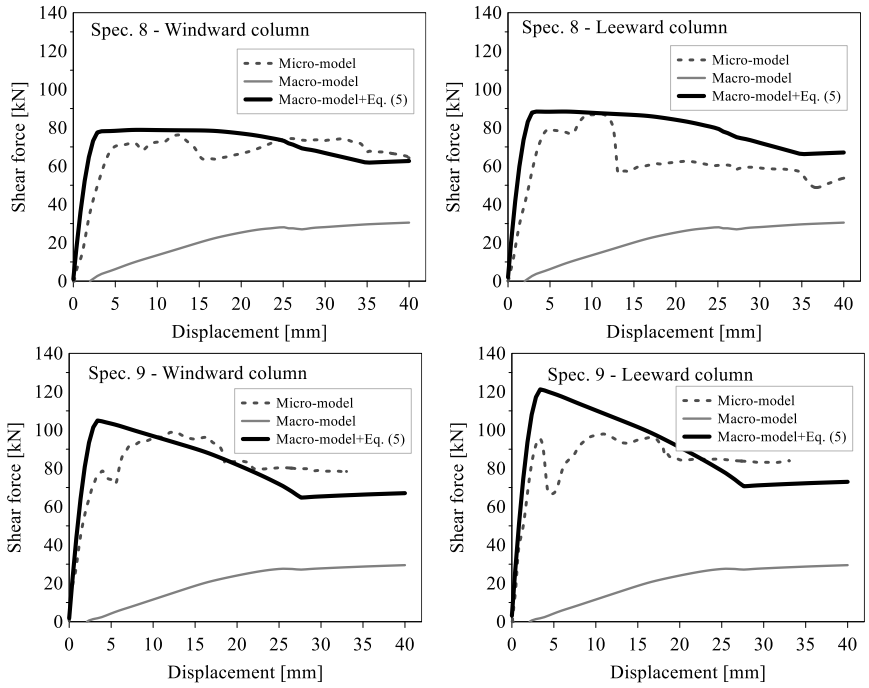

Fig. 13: Comparison between macro-model and micro-model predictions of shear demand at the windward and leeward column ends for Mehrabi & Shing [6] specimens: 8; 9.

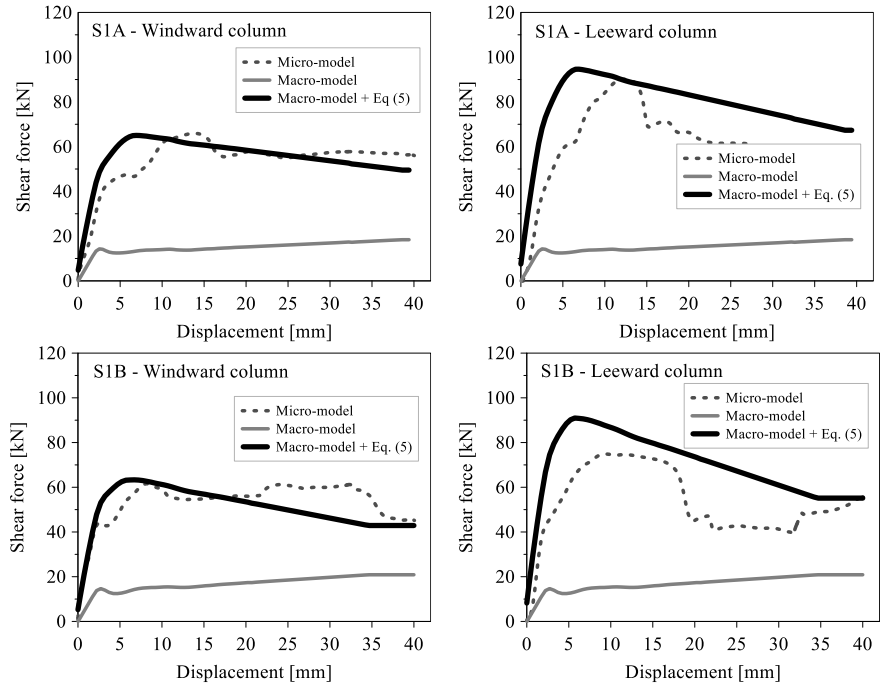

Fig. 14: Comparison between macro-model and micro-model predictions of shear demand at the windward and leeward column ends for Cavaleri & Di Trapani [2] specimens: S1A; S1B.

5 CONCLUSION

The additional shear demand resulting from the interaction between the frame and infill is crucial when assessing infill RC frames, as it may be responsible of local failures at the column ends and the joints. In this study, a refined micro-model for the infilled frame was formulated and realized with Open-Sees/STKO. The model validity was tested with four infilled frame specimens. The proposed micro-model enabled the evaluation of the internal forces distribution over the frame making use of a TCL script allowing the integration of the nodal forces across a specified cross-section. An analytical predictive model to estimate the additional shear demand when using the equivalent strut macro-modelling approach was also proposed. The latter relates the additional shear demand to the current axial force acting on the equivalent struts and also depends on the effective contact length of the infill with the frame (αl). Preliminary comparisons of the shear demand extracted from the micromodel with that estimated by the macromodel, and adjusted by the proposed analytical formulation, had quite good agreement assuming contact length values in the range 0.25l - 0.40l. This approach maintains the simplicity of the equivalent strut technique while ensuring accurate shear safety checks at the columns' ends. However, further research is necessary to determine more accurate contact length values and validate the proposed approach using a larger set of experimental tests.

ACKNOWLEDGEMENTS

This paper was supported by DPC-ReLuis 2022–2024, WP10, Subtask 10.1.2 - Non-structural masonry.

REFERENCES

[1] F. da Porto, M. Guidi, N. Dalla Benetta, F. Verlato, Combined in-plane/out-of-plane experimental behaviour of reinforced and strengthened infill masonry walls. *12th Canadian Masonry Symposium*, Vancouver, Canada, June 2–5, 2013.

[2] L. Cavaleri, F. Di Trapani, Cyclic response of masonry infilled RC frames: experimental results and simplified modeling. *Soil Dyn Earthq Eng,* **65**, 224–242, 2014.

[3] A. V. Bergami, C. Nuti, Experimental tests and global modeling of masonry infilled frames. *Earth Struct*, **9(2)**, 281–303, 2015.

[4] G. M. Verderame, P. Ricci, C. Del Gaudio, M.T. De Risi, Experimental tests on masonry infilled gravity- and seismic-load designed RC frames. *Proceedings of 16th international brick and block masonry conference (IBMAC)*, Padua, Italy, 2016.

[5] P. Morandi, S. Hak, G. Magenes, In-plane experimental response of strong masonry infills. *Eng Struct,* **156**, 503–521, 2018.

[6] A.B. Mehrabi, P.B. Shing, P.B., M.P. Schuller, L. Noland, Experimental evaluation of masonry-infilled RC frames. *J Struct Eng (ASCE),* **122(3)**, 228–237, 1996.

[7] A.B. Merhabi, P.B. Shing, Finite Element Modeling of masonry-infilled RC frames, *Journal of Structural Engineering*, **123**, 604-613, 1997.

[8] M. Papia, L. Cavaleri, M. Fossetti, Infilled frame: developments in the evolution of the stiffening effect of infills, *Structural Engineering and Mechanics*,**16(6)**, 675-694, 2003.

[9] G. Uva, D. Rafaele, F. Porco, A. Fiore, On the role of equivalent strut models in the seismic assessment of infilled RC buildings. *Eng Struct,* **42**, 83–94, 2012.

[10] A. Fiore, F. Porco, D. Rafaele, G. Uva, About the influence of the infill panels over the collapse mechanisms active under pushover analyses: Two case studies. *Soil Dyn Earthq Eng,* **39**, 11–22, 2012.

[11] L. Cavaleri, F. Di Trapani, P.G. Asteris, V. Sarhosis, Influence of column shear failure on pushover-based assessment of masonry infilled reinforced concrete framed structures: A case study. *Soil Dyn Earthq Eng,* **100**, 98–112, 2017.

[12] F. Di Trapani, M. Malavisi, Seismic fragility assessment of infilled frames subject to mainshock/ aftershock sequences using a double incremental dynamic analysis approach. *Bull Earthq Eng,* **17(1)**, 211–235, 2019.

[13] I. Koutromanos, A. Stavridis, P.B. Shing, K. Willam, Numerical modelling of masonry-infilled RC frames subjected to seismic loads. *Comput Struct,* **89**, 1026–1037, 2011.

[14] L. Cavaleri, F. Di Trapani, Prediction of the additional shear action on frame members due to infills. *Bull Earthq Eng,* **13(5)**, 1425–1454, 2015.

[15] I. Caliò, B. Pantò, A macro-element modelling approach of Infilled Frame Structures. *Comput Struct,* **143**, 91–107, 2014.

[16] R.R. Milanesi, P. Morandi, G. Magenes, Local effects on RC frames induced by AAC masonry infills through FEM simulation of in-plane tests. *Bull of Earthq Eng* **16(1)**, 4053– 4080, 2018.

[17] F. Di Trapani, A. Vizzino, G. Tomaselli, A.P. Sberna, G. Bertagnoli, A new empirical formulation for the out-of-plane resistance of masonry infills in reinforced concrete frames. *Eng Struct* **266**, 114422, 2022.

[18] F. Di Trapani, G. Bertagnoli, D. Gino, M.F. Ferrotto, Empirical equations for the direct definition of stress-strain laws for fiber-section based macro-modeling of infilled frames. *J Eng Mech* **144(11)**, 04018101, 2018.

[19] F. McKenna, G.L. Fenves, M.H. Scott, *Open system for earthquake engineering simulation*. University of California, Berkeley, CA, 2000.

[20] M. Petracca, F. Candeloro, G. Camata, *ASDEA Software STKO user manual*, 2017.

[21] M. Petracca, L. Pelà, R. Rossi, S. Zaghi, G. Camata, E. Spacone, E, Microscale continuous and discrete numerical models for nonlinear analysis of masonry shear walls. *Construction and Building Materials* **149**, 296-314, 2017.

[22] John Wiley&Sons (Editor), "*fib Model Code for concrete structures 2010*", 2013.

[23] D. D'Ayala, J. Worth, O. Riddle, Realistic shear capacity assessment of infill frames: comparison of two numerical procedures. *Eng Struct*, **31**, 1745–1761, 2009.

[24] L. Cavaleri, F. Di Trapani. Prediction of the additional shear action on frame members due to infills. *Bull Earthq Eng* **13**(5), 1425–1454, 2015.

[25] V. Bolis, A. Stavridis, M. Preti, Numerical investigation of the in-plane performance of masonry-infilled RC frames with sliding subpanels. *J Struct Eng,* **143(2)**, 04016168, 2017.